Product Yields from the Gas-Phase Ozonolysis
of Isobutene Using APCI-MS/MS

Dana Aljawhary

Supervisor: Professor Donald Hastie

Table of Contents

List of Figures

List of Tables

Abstract

The quantification of the products formed from the gas phase oxidation reaction of Isobutene by O_3 using Atmospheric Pressure Chemical Ionization Tandem Mass Spectrometry (APCI-MS/MS) was studied. Several products were identified, including Acetone, Methylglyoxal, Formic acid, Formaldehyde and Ketene. Other reactive products such as HO radicals, which can react with Isobutene, were suppressed by adding Cyclohexane as a scavenger. For product quantification, a correction was applied to the analyte signal in order to eliminate the dependence of the analyte ions concentration on the reagent ions concentration in the APCI source. Product yield measurements were carried out on Acetone in the presence and absence of the HO scavenger. The experimentally measured Acetone yield in the absence of the HO scavenger was 51%, which closely resembled the yield reported in the existing literature. However, a discrepancy was found between the Acetone yield in this work and the literature, when the HO scavenger was present. Calibration methods for the APCI-MS/MS and the resulting determination of the Acetone yield will be discussed.

1. Introduction

Alkenes are a class of volatile organic compounds (VOCs) which are present in trace levels in the atmosphere and involved in various atmospheric processes.[1] Gas phase oxidation reactions of alkenes are of atmospheric importance due to their role in the formation of photochemical air pollution, which has harmful impacts on human health and the environment.[1] The major atmospheric oxidants that take part in alkenes degradation are HO and NO_3 radicals and ozone.[1]A variety of chromatographic, spectroscopic and mass spectrometric techniques have been employed to study the kinetics and mechanisms involved in these oxidation reactions. Of these techniques, Atmospheric Pressure Chemical Ionization tandem Mass Spectrometry (APCI-MS/MS) has proven to be very powerful for on-line analysis, from which mechanistic and product structure information can be deduced.[2] However, when product quantification is required, spectroscopic and chromatographic methods, such as FTIR and GC-MS, are preferred over APCI-MS.[2] FTIR is a well established on-line quantification technique but it is limited to studies pertaining to small molecules.[2] Also, state of the art GC-MS instruments suffer from the low time resolution, especially during sample preparation and column separation.[2] Carrying out both qualitative and quantitative analyses in parallel using the APCI-MS can improve the understanding of alkene oxidation reactions as it overcomes the shortcomings of FTIR and GC-MS techniques. Employing the APCI-MS for on-line product quantification requires both sampling method development and understanding the ionization processes in the APCI source.

In this work, a reaction of a simple alkene with ozone has been studied to assess the potential of an APCI triple quadrupole MS for on-line product yield measurements. The alkene chosen was Isobutene because its ozonolysis products are unlikely to contribute to particle

formation making the analysis simpler.[1] Also, the gas phase products produced from this reaction are commercially available, which allows for their quantification. Even though HO is the most important daytime atmospheric oxidant, ozone was used in this work instead. Unlike O_3, HO must be produced by isopropyl nitrite (IPN) photolysis, which gets detected by the APCI-MS along with the photolysis products contributing to signal/noise reduction and adding more complexity to the reaction system. Still, the results from this simple ozonolysis reaction of isobutene would help in determining whether the instrument can be employed to quantify products of more complex reactions, including HO oxidation reactions.

1.1. Mechanism: Isobutene + O_3

The reactions of alkenes with ozone have received considerable attention in the past four decades,[3] especially after the discovery by Niki in 1987 of the direct production of HO radicals from these reactions.[4] The mechanism of the isobutene-O_3 reaction is illustrated in figure 1. The reaction proceeds by initial ozone addition to the double bond of isobutene forming an unstable five membered ring ozonide.[5] This is followed by a rapid decomposition of the ring structure into the primary carbonyl products and excited Criegee biradicals.[1] Since the structure of isobutene is asymmetric across the double bond, two channels leading to two different stable carbonyl products and two Criegee biradicals are possible. As shown in figure 1, each of the excited Criegee biradicals undergoes several pathways including, decomposition, rearrangement and stabilization channels. These are followed by the formation of stable secondary products.[1]
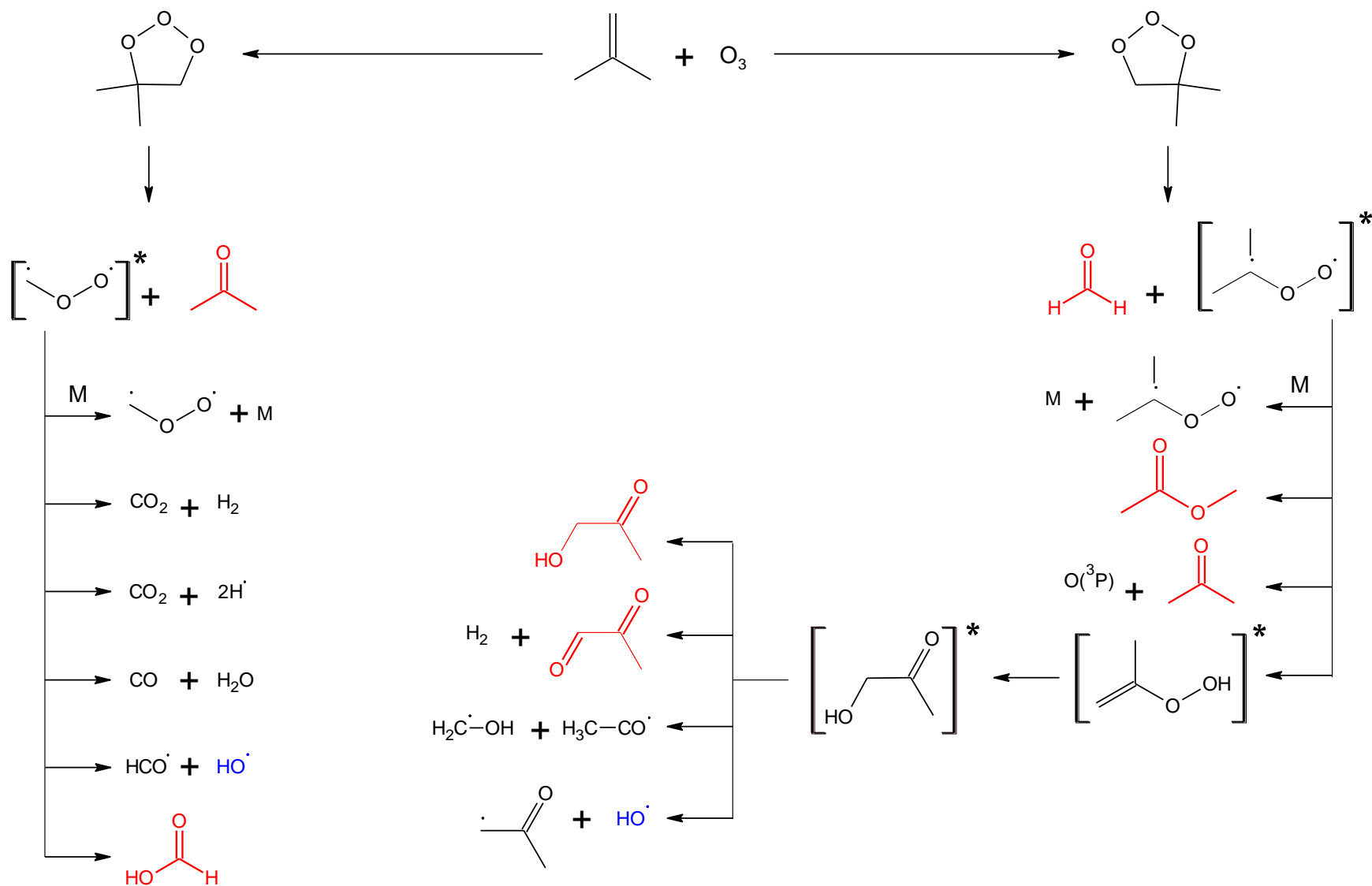
Figure 1: The Mechanism of gas phase ozonolysis of Isobutene. Stable products are highlighted in red.

1.2. HO scavenger

Other than the stable products that are formed in the isobutene-O_3 reaction, reactive products, such as HO radicals, are also formed. The reaction pathways leading to HO formation are shown in Figure 1. Since HO radicals are highly reactive, they can compete with ozone for isobutene, leading to complicated reactions. A commonly used scavenger to suppress the HO level in the ozonolysis reactions of alkenes is cyclohexane.[6] Cyclohexane is an alkane and does not react with ozone since it is lacking a double bond. When it is present in excess, it reacts with HO radicals through the hydrogen abstraction reaction pathway shown in figure 2.[1]
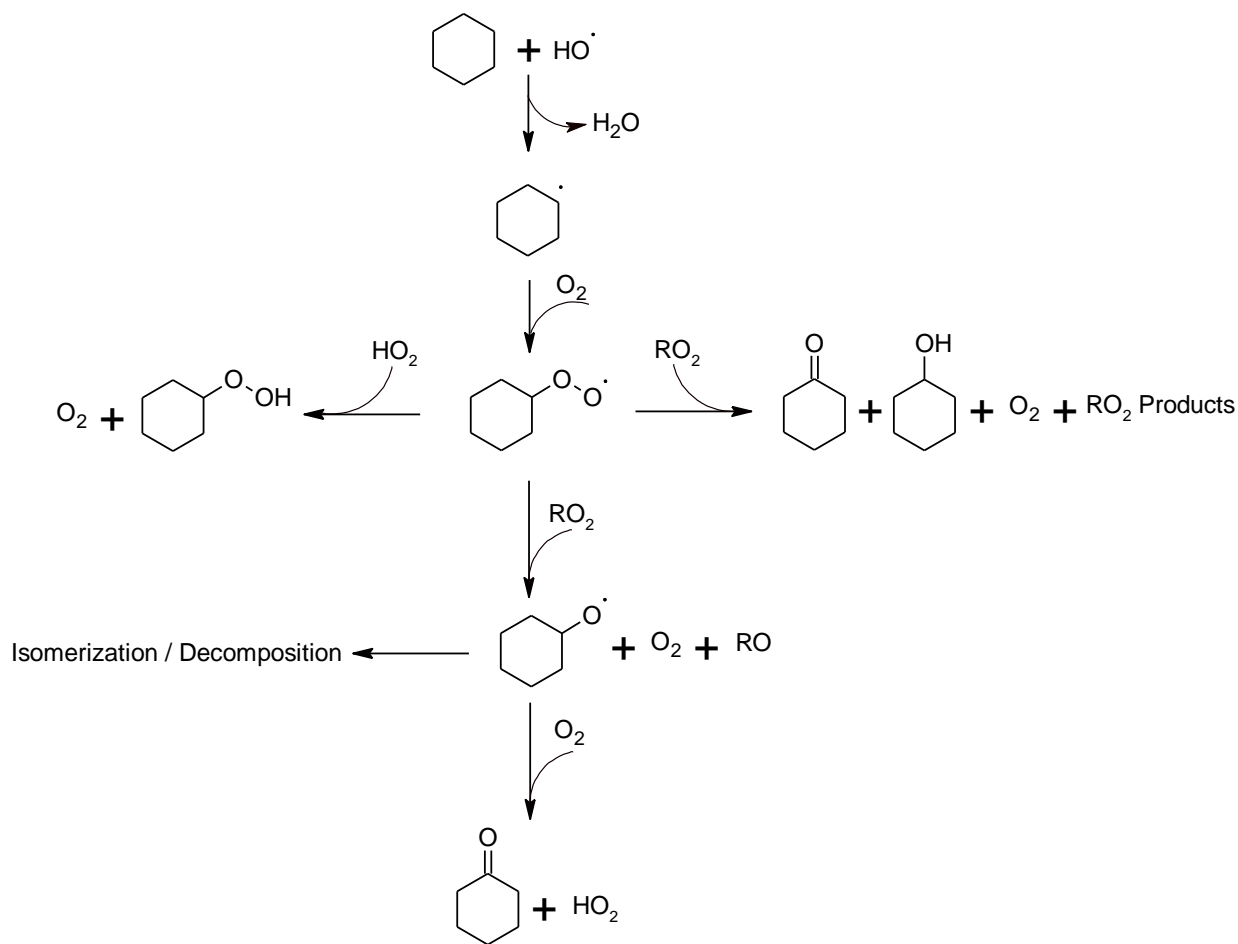
Figure 2: Reaction pathways for Cyclohexane oxidation by HO.

4

1.3. APCI ionization

In APCI-MS, ionization of the analyte (VOC) takes place by a proton transfer reaction in the gas phase from protonated reagent ions to the neutral analyte. The most commonly used reagents ions are protonated water cluster ions, $H^+(H_2O)_n$ (R1).

$$H^+(H_2O)_n + VOC \longrightarrow VOCH^+(H_2O)_m + (n-m)H_2O \quad \text{(R1)}$$
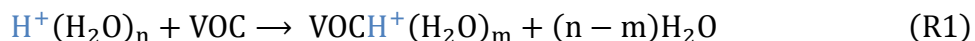
The spontaneity of R1 can be evaluated using the gas phase basicity (GB), which is defined as the negative of the Gibbs free energy change (ΔG^o) of R2:[7]

$$X_{(g)} + H^+_{(g)} \longrightarrow XH^+_{(g)} \quad \text{(R2)}$$

Although, ΔG^o is the correct physical quantity that determines reaction spontaneity, proton affinity (PA), which is the negative of the enthalpy change of R2,[7] is sometimes used instead.[8] This is due to the fact that the entropy change in R2 is small and show little variation among a wide range of reactions.[8]

It is essential to note that the GBs and PAs of about 1700 molecules, radicals and neutral atoms have been evaluated by Hunter and Lias, allowing for the spontaneity of R1 to be easily evaluated.[7] Their results have shown that there is a close proximity between PA(VOC) and PA(H_2O), leading to an exothermic R1 with an energy small enough to keep the VOC intact.[8] As a result, the proton transfer reaction in R1 is almost always non-dissociative.[8]

It has been reported that several factors; such as the abundance of the reagent ions ($H^+(H_2O)_n$), their cluster size distribution, and the PA of the analyte, have critical impact on the extent of VOCs ionization (R1) and the APCI-MS sensitivity.[9] As a result, accounting for such factors is vital when VOCs quantification is desired.

2. Experimental

Three kinds of experiments were conducted in order to complete the yield measurements of the Isobutene-O_3 reaction products: Calibration, Isobutene reaction with O_3 and Control experiments. For all the experiments, an APCI triple quadrupole mass spectrometer (PE Sciex API 365) was used for detection.

2.1. Calibration

The experimental set up used for the calibration experiments is shown in figure 3 (next page). A purified AADCO air, at a flow of 10 L/min, was used to dilute the standards. The standards used were acetone (Sigma-Aldrich, purity ≥99.9%) 4% V/V% water solution and Methylglyoxal solution (Sigma-Aldrich, 40% aqueous solution). A 50 μL syringe (705N Hamilton) filled with the standard was inserted into the dilution air stream through a septum. Different concentrations of the standards were obtained by varying the syringe flow rate using a syringe pump (Harvard Apparatus Holliston MA). Only 0.56 L/min, measured using a flowmeter, of the diluted standard was allowed to enter the ion source and the rest was vented out. Air humidifier was also admitted to the ion source with a flow rate of 1 L/min. This is to ensure that enough reagent ions ($H^+(H_2O)_n$) are present in the APCI ion source to ionize the standard. The exhaust line connected to the APCI source was at atmospheric pressure.

Two 3-point calibrations were completed for each experiment, one before and one after the Isobutene-O_3 reaction and Control experiments (described next). The concentrations used for acetone calibrations were 0.24, 0.71 and 1.2 ppm. Methylglyoxal calibration was not successful (See Methylglyoxal section) and a modification to the set up had to be made, where the air stream entering the ionization region in the APCI source was heated using a heated nebulizer.
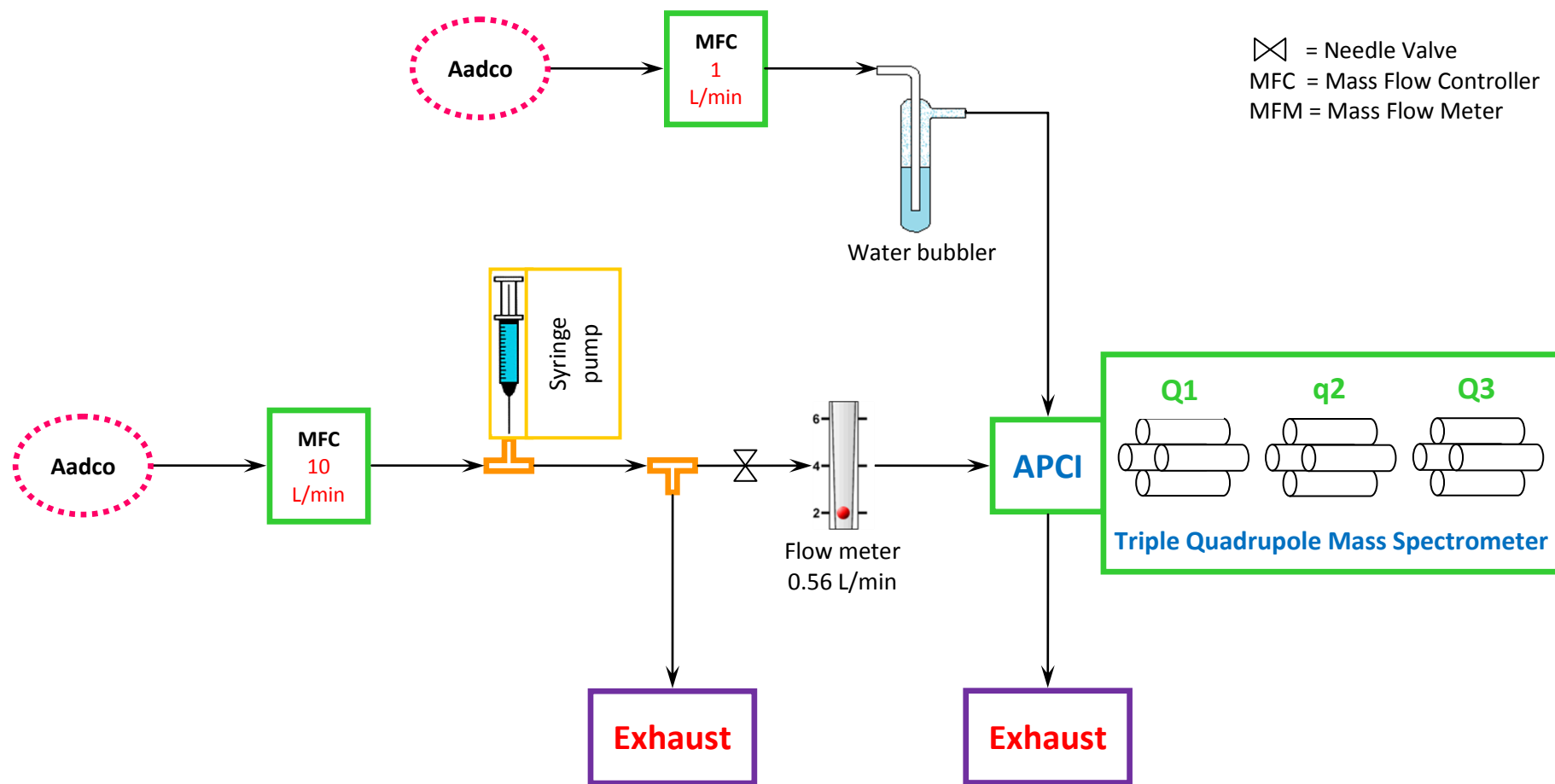
Figure 3: Experimental set up for the calibration experiments.

2.2. Reaction of Isobutene with O_3

The system used to carry out the reaction of Isobutene and O_3 has been previously used to study gas phase oxidation reactions of aromatic hydrocarbons by HO radicals. Earlier, air flows of Isopropyl nitrite (IPN), NO and the hydrocarbon were admitted into a 2.7 L cylindrical Pyrex flow reactor. The flow reactor was irradiated by a UV lamp in order to initiate the photolysis of IPN, which was the source of HO radicals. A Counter Flow Membrane Denuder (CFMD) was connected to the flow reactor upstream in order to separate the gas and particle phase products. Then, APCI MS/MS (TAGA 6000 E) was used for the detection.[9]

In this study, this system had to be modified in order to carry out isobutene ozonolysis reactions. A schematic diagram of the experimental set up that was used to carry out this reaction is illustrated in figure 4. The reactants, Isobutene and O_3 were admitted to the flow reactor, where the ozonolysis reaction took place. A gas standard of pure Isobutene (Air Liquide, 99.0% wt%) was diluted with purified AADCO air in a two stage dilution system, which was specifically assembled for this study, to achieve a concentration of 1.5 ppm in the flow reactor. To obtain a 15 ppm concentration of ozone, attempts were made using UV lamps were not successful. As a result, ozone had to be generated by electric discharge in a 0.06 L/min AADCO flow using an ozonator (NOx analyzer, model 8840; Monitor Labs Inc.). The concentration of ozone was measured using an ozone monitor (Dasibi, model 1003-RS).The concentration obtained from the ozonator was approximately 180 ppm in the flow reactor, which was significantly higher than the desired concentration. For this, a modification had to be made in order to reduce the amount of O_3. Figure 5, shows a schematic diagram of the apparatus used for O_3 destruction and dilution. From the ozonator outlet, the flow was split into two lines; one goes
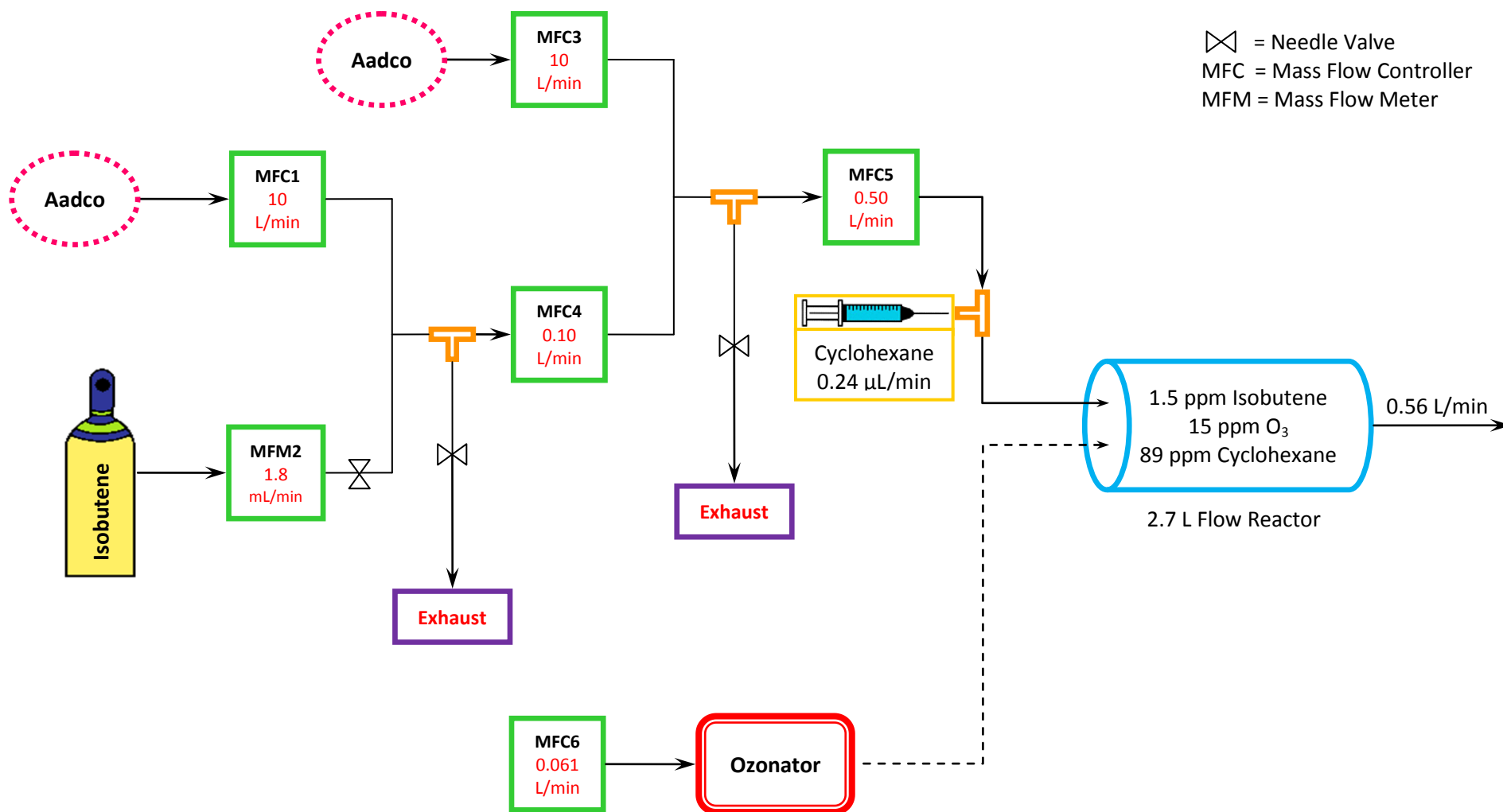
Figure 4: A schematic diagram of the experimental set up that was used to carry out the reaction of Isobutene with Ozone in the flow reactor. See figure 5 for illustration about the dashed line)
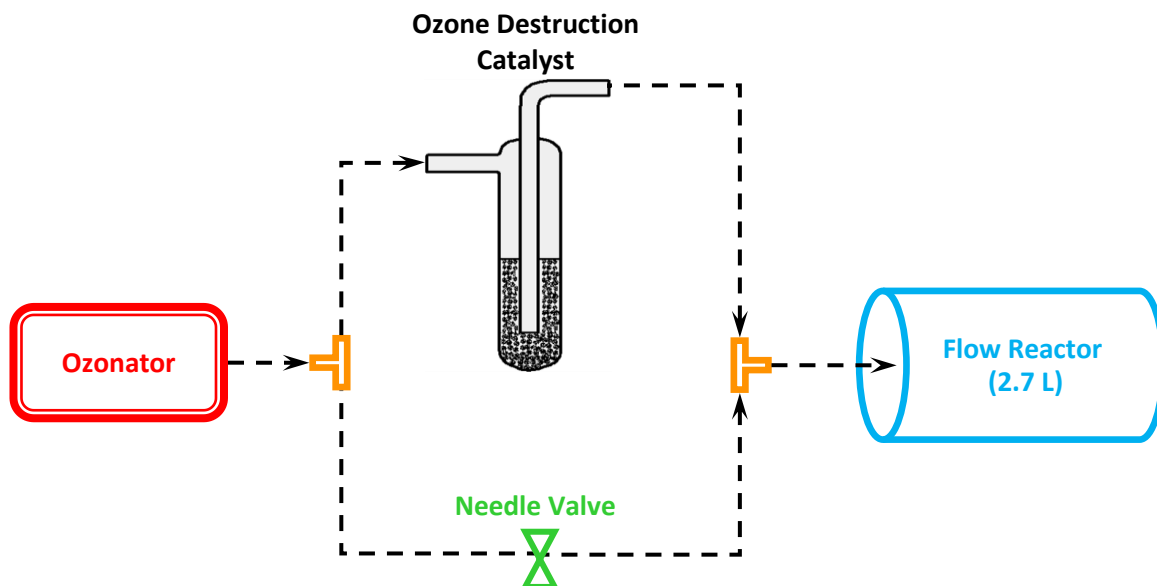
Figure 5: Ozone suppression and dilution set up (the dashed line in figure 4). The destruction catalyst contains MnO_2-coated charcoal.

through a needle valve and another goes through an ozone destruction catalyst. This catalyst was made of a glass trap filled with MnO_2-coated charcoal, which catalyzes the conversion of ozone to O_2. The split flows were then joined upstream. The concentration of ozone was varied by adjusting the flow through the needle valve shown in figure 5. By using this ozone destruction system, a concentration of 15 ppm of ozone was obtained in the flow reactor.

In addition to Isobutene and O_3, the HO scavenger, cyclohexane, was introduced into the flow reactor. A 50 μL syringe (705N Hamilton) filled with the cyclohexane (Caledon lab, purity 99%) was inserted into the flow carrying Isobutene through a septum. A concentration of 89 ppm in the flow reactor was obtained by setting the syringe pump (Harvard Apparatus Holliston MA) at a flow rate of 0.24 μL/min. The reaction was carried out in the presence and absence of cyclohexane and the reaction products were detected under each of these conditions.

The flow rate of the air carrying the reagents was adjusted such that a residence time of 4.8 min inside the flow reactor was achieved. This allowed 71% or the reaction to proceed toward completion.

2.3. Control Experiment

This experiment was performed to test the effect of using excess cyclohexane on acetone measurement. The same experimental set up for the Isobutene-O_3 reaction was used to carry out the control experiment with slight modification. Isobutene flow from the cylinder (MFM2) was blocked and a second syringe pump was used to inject acetone (the same standard used for the calibrations) in series with cyclohexane through the line connecting MFC5 to the flow reactor (Figure 4). The acetone pump was sat at a flow rate such that a 0.43 ppm of acetone was obtained in the flow reactor. Acetone signal was acquired using the APCI-MS, in the presence and absence of cyclohexane from the flow reactor.

2.4. Triple Quarupole MS

The APCI triple quadrupole mass spectrometer (PE Sciex API 365) consists of three quadrupoles arranged in series. Each of the quadrupoles is made up of four rods mounted in a square configuration as shown in figure 6. The APCI-MS was operated using three scan modes, which will be discussed briefly in the next subsections.
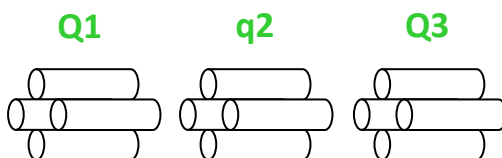
Figure 6: Schematic of a Triple Quadupole MS.

2.4.1. Q1MS

In the Q1MS scan mode, the Q1 is set to scan the ions entering from the APCI source region. The q2 and Q3 are set to keep the ions in focus until they reach the detector. The Q1MS spectrum shows all the ions that are formed in the APCI source, which have *m/z* within a selected *m/z* range.

2.4.2. MS/MS

The MS/MS (or product ion) scan helps in obtaining structure information about the analyte of interest. In this scan, the Q1 act as a mass filter, where it selects one ion (precursor ion) that is emerging from the source region and allows it to pass through to the q2. All the other ions are filtered out. In the q2, the selected ion undergoes collisions with a collision gas which induces its fragmentation. The extent of precursor ion fragmentation can be controlled by varying the collision energy. The fragments formed due to collision (product ions) as well as any remaining precursor ions are scanned in the Q3.

2.4.3. SRM

The Selected Reaction Monitoring (SRM) scan is very similar in operation to the MS/MS scan mode. In fact, the only difference is in the Q3 function, which operates as a mass filter, selecting only one of the product ions formed by the Collision Induced Dissociation (CID) and allowing that only ion to pass through to the detector. This scan was used to obtain all the quantitative measurements performed in this work as it is characterized by the high selectivity and signal/noise.

3. Results and Discussion

3.1. Product Identification

The reaction was carried out with and without the HO scavenger, cyclohexane. Figure 7, shows the background subtracted Q1MS spectra of the reaction products under both of these conditions. Since the focus of this project was to determine product yields rather than product identification, differences in the product distribution between the two spectra in Figure 7 were not of interest. However, the products formed in the presence of cyclohexane had to be identified before any product quantification experiments could be carried out.
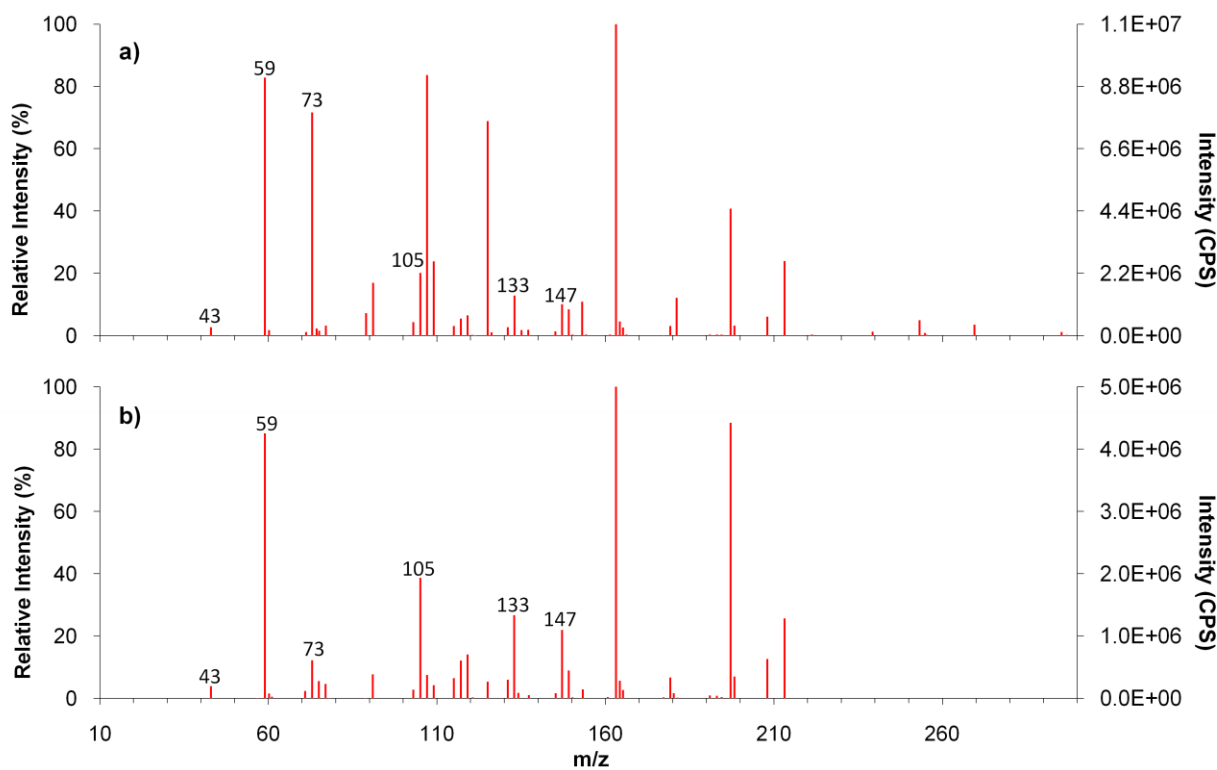
Figure 7: Background subtracted Q1MS spectra of the isobutene-O_3 reaction products: a) without the HO scavenger. b) with the HO scavenger.

The mechanism discussed earlier suggests that potential products include: H_2, CO, CO_2, Formaldehyde, Acetone, Methylgloxal, Hydroxyacetone, Methyl acetate, Formic acid and Methanol. Table 1 lists the proton affinities (PAs) of the expected products. The PAs of H_2, CO,

13

Table 1: Proton affinity values for potential products from the ozone-isobutene reaction.[7]

Compound	Proton affinity (kJ/mol)
H_2O	691.0
H_2	422.3
CO	594.0
CO_2	540.5
Formaldehyde	712.9
Acetone	812.0
Methylgloxal	-
Hydroxyacetone	-
Methyl acetate	821.6
Ketene	825.3
Formic acid	742.0
methanol	754.3

CO_2 are less than the PA of water. Thus, the ionization of these compounds will not take place in the APCI source. The PAs of methylglyoxal and hydroxyacetone are not reported, still, those compounds are oxygen bases and their PAs are expected to be in the PA range of organic compounds with similar functional groups. Methylglyoxal has two carbonyl groups, while hydroxyacetone has one carbonyl and one hydroxyl group. Those functional groups resemble the ones found in acetone, formaldehyde and methanol, listed in table 1. Thus, proton transfer reaction from the reagent ions to methylglyoxal and hydroxyacetone is expected to proceed in the ion source.

3.1.1 Acetone (MW = 58 u)

Several ions, related to acetone (AC), were observed in the experimental Q1MS spectrum. These included the protonated acetone (ACH$^+$), the protonated acetone water cluster (ACH$^+$(H_2O)) and the protonated acetone dimer (AC$_2$H$^+$) ions at *m/z* 59, 77 and 117,

respectively. Acetone was identified as a reaction product by comparing the MS/MS spectra, of the precursor ion of *m/z* 59, obtained from the isobutene-O₃ reaction with that of acetone standard. As shown in figure 8, the reaction product and the acetone fingerprint MS/MS spectra are consistent with each other, when the fragmentation pattern and the product ions ratios are compared. This confirms that acetone is a product from the reaction of isobutene with ozone.
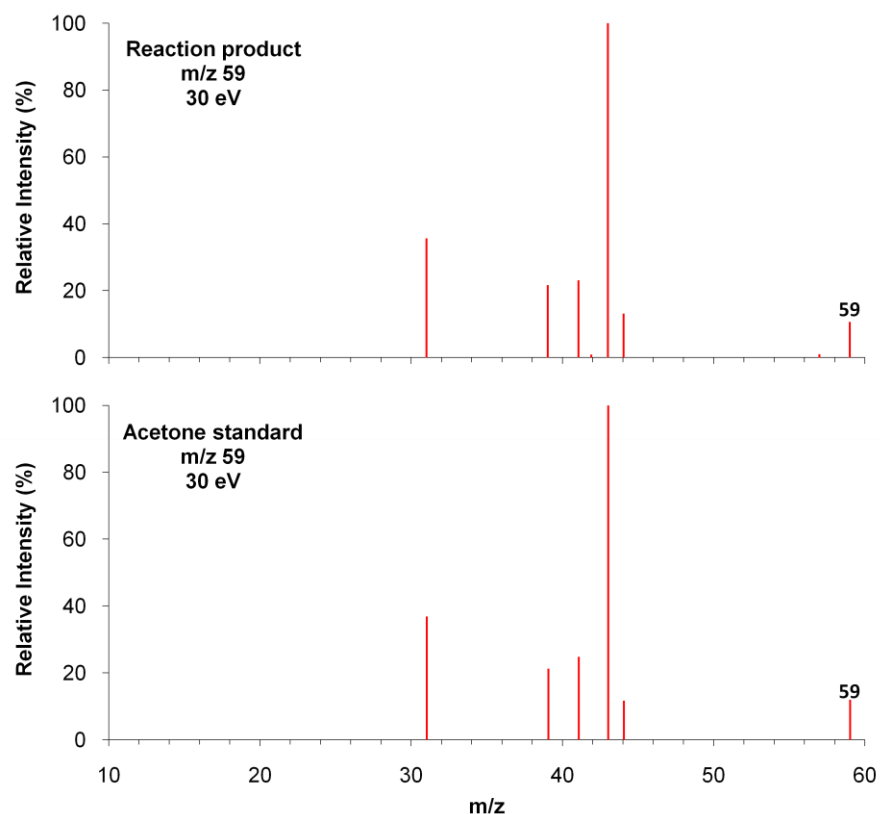
Figure 8: MS/MS spectra of precursor ion *m/z* 59 from the isobutene-O₃ reaction (top) and acetone standard (bottom) using collision energy of 30 eV.

3.1.2 Methylglyoxal (MW = 72 u)

Methylglyoxal (MG) is commercially available only as a solution in water (40%), where it is present in the hydrated forms (see section 3.2.4). As a result, it was not possible to compare the reaction product MS/MS spectra to MG standard spectra. Instead, MG was identified by interpreting the fragmentation pattern of precursor ions, which were hypothesised to be MG

15

related ions. These precursor ions include MGH^+, $MGH^+(H_2O)$, $MGH^+(H_2O)_2$ and $MG_2H^+(H_2O)_2$ at m/z 73, 91, 109 and 181, respectively. Table 2 shows the fragmentation pattern observed from the MS/MS spectrum of precursor ion m/z 73. The observed water loss is

Table 2: A list of the product ions observed in the MS/MS spectrum of precursor ion m/z 73 at 20 eV.

Product ion (m/z)	Loss	
	mass (u)	Interpretation
58	15	CH_3
55	18	H_2O
45	28	CO
43	30	CH_2O
31	42	C_2H_2O

an indicative of at least one oxygen atom in the structure. Also, the loss of CO at m/z 45 hints at a carbonyl group. This carbonyl group can either be part of a ketone or an aldehdye. However, there is also a loss of a methyl group (table 2), which suggests that the structure can either be:

$$MW(X) = 28 \text{ u} \qquad MW(X) = 29 \text{ u}$$
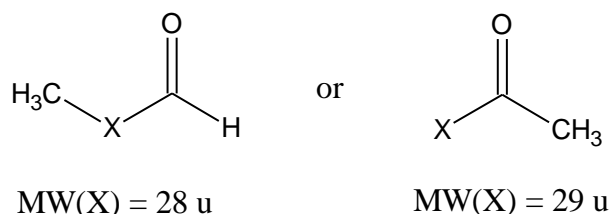
Mass 28 u corresponds to a $-C=O$ or $-CH_2-CH_2-$ group, while mass 29 u corresponds to an aldehyde ($O=C-H$) or an ethyl $-CH_2-CH_3$ group. Based on the mechanism discussed earlier, the maximum number of carbons a product can have should not exceed three carbons. As a result, it is very unlikely to form butanal from the reagent isobutene and the ethyl group can be excluded. This suggests that the structure has two conjugated carbonyl groups, which is consistent with the MG structure.

3.1.3 Ketene (MW = 42 u)

The Q1MS spectrum (figure 7) shows a peak at m/z 43. MS/MS experiments were not carried out to identify the structure of this ion. As a result, it might be argued that the precursor ion at m/z 43 may correspond to several reaction products with the same nominal mass. However, the elemental composition of the reagents, isobutene and ozone, includes carbon, oxygen and hydrogen. With this elemental composition, only products with the chemical formula, C_2H_2O, can have a nominal mass of 42 u. Candidates with this chemical formula are:

| ketene | oxirene | ethynol |
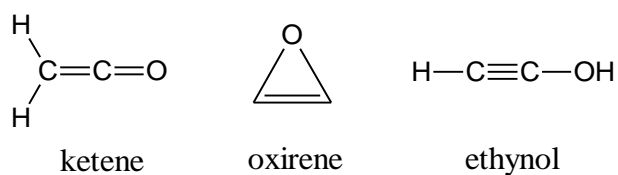
The formation of oxirene and ethynol from the reaction of isobutene with ozone has not been reported in the literature, unlike ketene, which has been detected and measured.[5] In fact, even if oxirene and ethynol were formed from the reaction, both are highly unstable and rapidly rearrange to form ketene.[10, 11] Therefore, the peak at m/z 43 was assigned to ketene.

Ketene was also detected as part of ion clusters, which were composed of different reaction products. Examples of these clusters are listed in table 3.
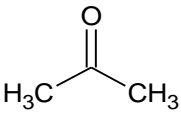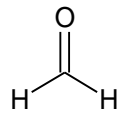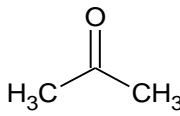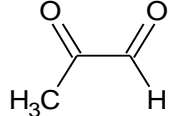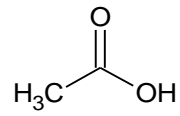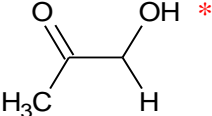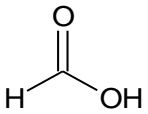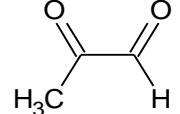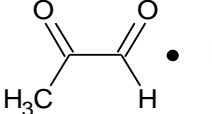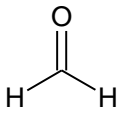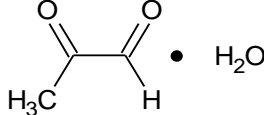
3.1.4 Other products

The rest of the reaction products from the isobutene-O_3 reaction did not show unique ions in the Q1MS spectrum so that they could not be identified in the same way as was done for MG. A combination of different reaction products clustering together appeared at the same m/z instead. Therefore, identification based on interpreting the fragmentation pattern of a single product was not possible. The identification of these products was based on their nominal masses

and proposed structures were confirmed by comparison to the existing literature.[1, 5] This was achieved using the MS/MS scan mode at the lowest collision energy (5 eV) in order to ensure that dissociation of the cluster ion complex was only due to disruption of weak Van Der Waals interactions or hydrogen bond breakage.

Table 3 shows the reaction products that were identified using this method, which includes: formaldehyde, methanol, formic acid, acetic acid, hydroxyacetone (or methyl acetate). Confirmation of the identity of these products requires additional resources, such, as an MS^n scan, which is not a feature of standard triple quadrupole mass spectrometers.

Table 3: Composition of three precursor ions obtained using MS/MS experiments at 5 eV. The product ions observed for each precursor ion are listed with the associated losses and their interpretation.

Precursor Ions								
m/z 105			**m/z 133**			**m/z 147**		
Product ion (m/z)	Loss		Product ion (m/z)	Loss		Product ion (m/z)	Loss	
	Mass (u)	Interpretation		Mass (u)	Interpretation		Mass (u)	Interpretation
87	18	H_2O	115	18	H_2O	89	58	$H_3C-CO-CH_3$ (acetone)
75	30	$H_2C=O$ (formaldehyde)	75	58	$H_3C-CO-CH_3$ (acetone)	75	72	$H_3C-CO-CHO$ (methylglyoxal)
73	32	H_3C-OH	73	60	$H_3C-CO-OH$ (acetic acid)	73	74	$H_3C-CO-CH(OH)H$ *
59	46	$H-CO-OH$ (formic acid)	61	72	$H_3C-CO-CHO$ (methylglyoxal)	57	90	$H_3C-CO-CHO$ (methylglyoxal) • H_2O
43*	62	$H_2C=O$ (formaldehyde) • H_3C-OH	43*	90	$H_3C-CO-CHO$ (methylglyoxal) • H_2O	43*	104	-

*Methyl acetate is also possible.
*Ketene.

3.2. Calibration

Out of all the products that have been identified, only Acetone (AC), Methylglyoxal (MG) and Ketene formed unique ions (ie. not clustering with other reaction products) in the APCI ion source. That was one of the important conditions that had to be satisfied prior to any quantification attempts. Also, liquid standards of the products had to be commercially available so that calibrations could be carried out. Since Ketene is highly reactive and is present in the gas phase at room temperature, quantitative measurements of Ketene were not made. However, standards for Acetone were available in pure liquid form and as a solution in water (40%) for Methylglyoxal. As a result, calibration attempts for these two products were performed and investigated.

3.2.1. Signal Correction

Several problems have been encountered when using APCI-MS for quantitative measurements. Conventional calibration curves, where the raw signal is plotted against the concentration of the analyte, have been found to have poor repeatability during the course of experiments, small linear range and a reversal in the sensitivity at high analyte concentration. In order to obtain better calibrations, the ionization process in the APCI source had to be further understood.

As mentioned earlier, ionization takes place in the APCI source by a proton transfer reaction from protonated water cluster ions to the neutral analyte.

$$H^+(H_2O)_n + A \longrightarrow AH^+(H_2O)_m + (n-m)H_2O \qquad \text{(R3)}$$
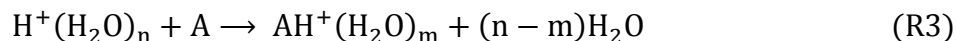
The kinetics and thermodynamics of this reaction have been thoroughly studied.[12, 13] R3 proceeds rapidly under atmospheric pressure so that equilibrium conditions are reached in the ion source

for compounds with proton affinities lower than 837 kJ/mol.[13] A class of compounds that fits

under this category is that of oxygen bases, which includes oxygenated VOCs that are formed

from VOC oxidation reactions.[13] The equilibrium constant expression for R3 can be used to

obtain a relation between the concentration of the analyte [A] and the protonated analyte ions

$[AH^+(H_2O)_m]$,[13]

$$K = \frac{[AH^+(H_2O)_m] \times [H_2O]^{n-m}}{[H^+(H_2O)_n] \times [A]} \tag{E1}$$

By rearranging,

$$[A] = \frac{[AH^+(H_2O)_m]}{[H^+(H_2O)_n]} \times \frac{[H_2O]^{n-m}}{K} \tag{E2}$$

Assuming that the concentration of the ions in the APCI ion source is proportional to their

corresponding intensities and that the concentration of water vapour remains constant,[13]

$$[A] = \frac{I_{AH^+(H_2O)_m}}{I_{H^+(H_2O)_n}} \times C \tag{E3}$$

This expression (E3) is valid when the ion intensity ratio is representative of the equilibrium ion

concentration ratio. However, a declustering gas (interface gas), which is located between the

quadrupoles and the ion source, dehydrates the ion clusters coming from the ion source

disturbing the equilibrium ion distribution.[14] As a result, information regarding the hydrated

analyte (or reagent) ion concentration in the APCI source at equilibrium cannot be directly

obtained from their corresponding intensities.[14] Fortunately, a mathematical model has been

derived by Kebarle, which relates the sum of the hydrated ion $(AH^+(H_2O)_m)$ intensities to the

sum of their concentrations for a particular analyte (A).[13] This model allows re-evaluating E3 to,

$$[A] = \frac{\sum I_{AH^+(H_2O)_m}}{\sum I_{H^+(H_2O)_n}} \times C \tag{E4}$$

E4 shows the dependence of the analyte ions concentration (or signal) on the concentration of the

analyte [A] and the concentration of the reagent ions $(H^+(H_2O)_n)$. As long as the reagent ions concentration remains constant, calibrations using the raw intensity of the analyte ions are valid. However, depletion in the reagent ions concentration is usually observed in the presence of high concentration of analyte or in the presence of analytes with high proton affinities. In this case, a correction has to be applied to the raw analyte signal using E4 in order to eliminate any dependence of the analyte ions concentration on the reagent ions concentration.

Another ionization reaction in the APCI source involves the formation of a protonated analyte dimer ion. This proton transfer reaction is represented in reaction 2 (R4).

$$H^+(H_2O)_n + 2A \rightleftharpoons A_2H^+(H_2O)_m + (n-m)H_2O \tag{R4}$$
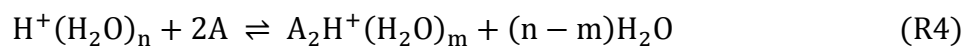
Analogous expressions to E3 and E4 can be derived for the protonated dimer ions based on the equilibrium conditions in the APCI source,

$$[A] = \sqrt{\frac{I_{A_2H^+(H_2O)_m}}{I_{H^+(H_2O)_n}}} \times C \tag{E5}$$

$$[A] = \sqrt{\frac{\sum I_{A_2H^+(H_2O)_m}}{\sum I_{H^+(H_2O)_n}}} \times C \tag{E6}$$

Note that E6 was not derived by Kabarle or reported in literature. It was assumed that the derivation of the dimer ions $(A_2H^+(H_2O)_m)$ expression (E6) would follow the same mathematical formulations, which were applied to derive the protonated monomer ions $(AH^+(H_2O)_m)$ expression (E4).

Previous work has shown that using E4 and E6 has a great impact on improving the linear range of calibrations. Also, the dependence of the analyte ions concentration on the reagent ions concentration, which causes an inverse response to increasing analyte concentration, is

22

eliminated. Thus, the correction of the analyte signal by dividing it by the reagent ion signal was utilized to obtain quantitative measurements of Acetone and Methylglyoxal. All the calibration ion signals were obtained using the SRM scan mode.

3.2.2. Acetone

Since one of objectives of this project was to quantify the acetone produced from the isobutene-O_3 reaction, two calibrations were carried out; one before the reaction (1st) and another after the reaction (2nd). A list of the SRM precursor $\rightarrow$ product ion pairs, which were followed for acetone measurements, is given in table 4. In addition to the acetone ion pairs, the intensities of the APCI reagent ions were also followed so that corrections using E4 and E6 can be applied.

Table 4: A list of acetone and proton SRM precursor $\rightarrow$ product ion pairs that were followed for calibrations.

	Precursor ion (*m/z*)		Product ion (*m/z*)
Acetone (AC)	ACH^+	59	41
	$ACH^+(H_2O)$	77	59
	AC_2H^+	117	59
Proton	$H^+(H_2O)_3$	55	37
	$H^+(H_2O)_2$	37	19

Acetone calibrations were carried out at two collision energies (CE), 5 eV and 20 eV, in order to obtain a good signal/noise for all ions. To illustrate, at 5 eV only *m/z* 77 and 117 showed high signal/noise, while *m/z* 59 signal/noise was comparably very low at the same CE (fig. 9). That was due to the fact that the acetone molecule has a rigid structure and product ion formation from the precursor *m/z* 59 by CID requires covalent bond breakage. On the other hand, in order to observe product ion signal from precursor ions *m/z* 77 and 117, only weak bond breakage is required.

Figures 9 and 10 show the calibration curves obtained for the three acetone ions at 5 and 20 eV. In the left pane, the raw signal is plotted against the acetone concentration, while in the right pane; the corrected acetone signal is plotted as a function of acetone concentration. The depletion in the proton signal as a result of increasing acetone concentration is demonstrated in figure 11. The slopes of the 1st and 2nd calibration lines for m/z 59 curves get closer to each other in magnitude, when the signal is corrected using E4. The calibration curves for both m/z 77and 117 show curvature when the raw signal is used to obtain the calibrations. Enhancement in the linearity of these two curves can be seen when the relative signal is used instead.

A better assessment of the calibration curves shown in figures 9 and 10 can be made if the relative standard deviations of the slopes (%S_m) are compared. A summary of the %S_m is given in table 5. The %S_m of the curves obtained by plotting the relative signal is dominantly lower than the %S_m of the corresponding curves, where the raw signal is plotted as a function of acetone concentration. One exception is the 1st 5 eV m/z 59 curves, which could be due to the poor signal/noise at 5 eV for m/z 59 as discussed earlier. Based on the overall quality of the corrected calibration curves, the correction method was adopted for quantitative measurements.

Table 5: Relative errors in the slope (% S_m) of the calibration curves shown in figures 9 and 10. Yellow shading is an indicative of where higher % S_m exists.

CE	Calibration	% S_m					
		m/z 59		m/z 77		m/z 117	
		Signal	Relative	Signal	Relative	Signal	Relative
5ev	1st	1.6	5.2	6.5	2.1	16	0.80
	2nd	3.2	0.97	4.7	0.50	17	0.30
20ev	1st	3.1	2.1	6.5	0.81	17	0.071
	2nd	5.4	1.1	7.1	2.5	15	2.0

Figure 9: Acetone calibration curves using three precursor → product ion pairs at **5 eV**. Raw signal and relative signal of the acetone pairs are plotted against the concentration of acetone in the left and right pane, respectively. Each graph includes the 1st and 2nd calibration curves. Standard errors are listed in table 7 in the appendix.
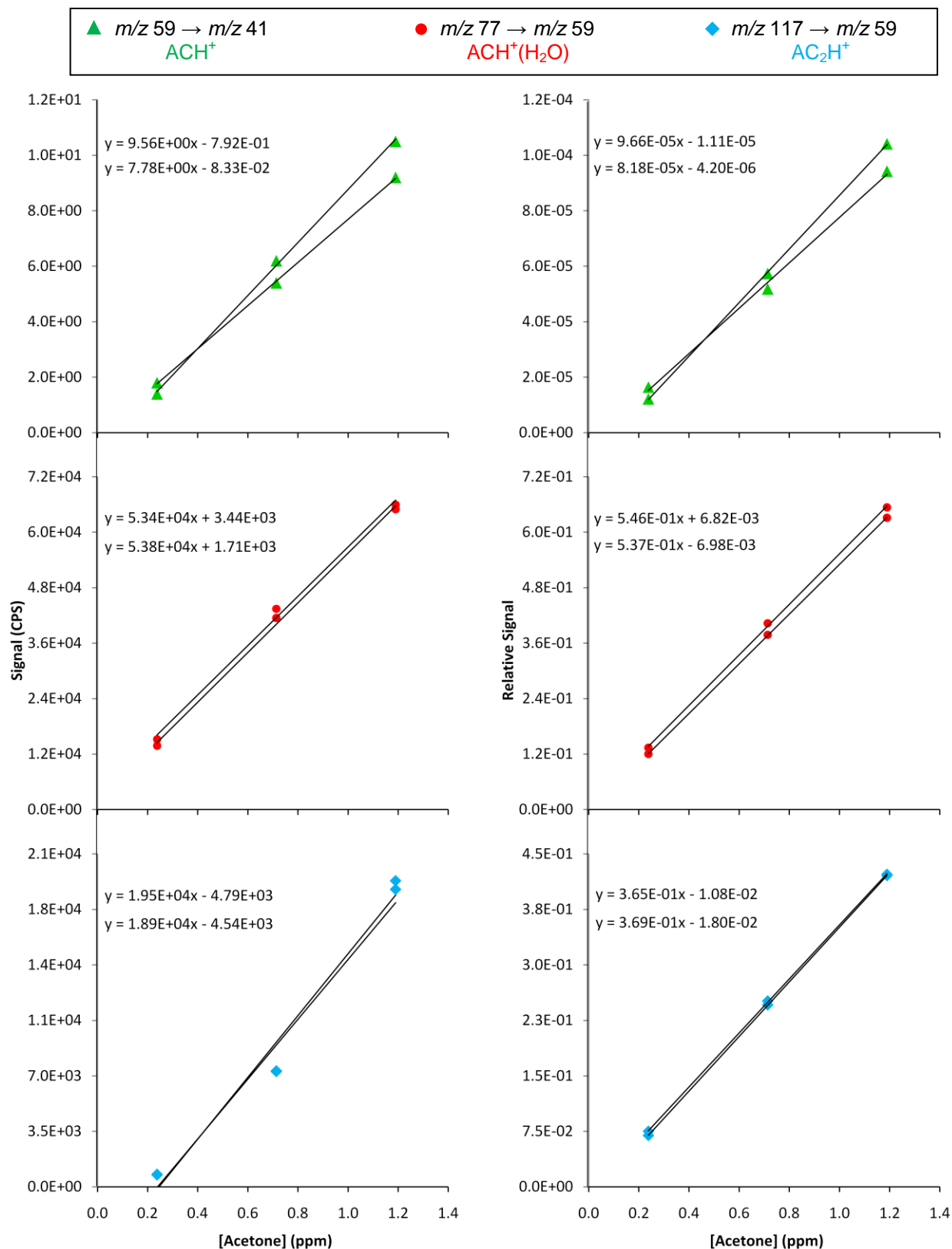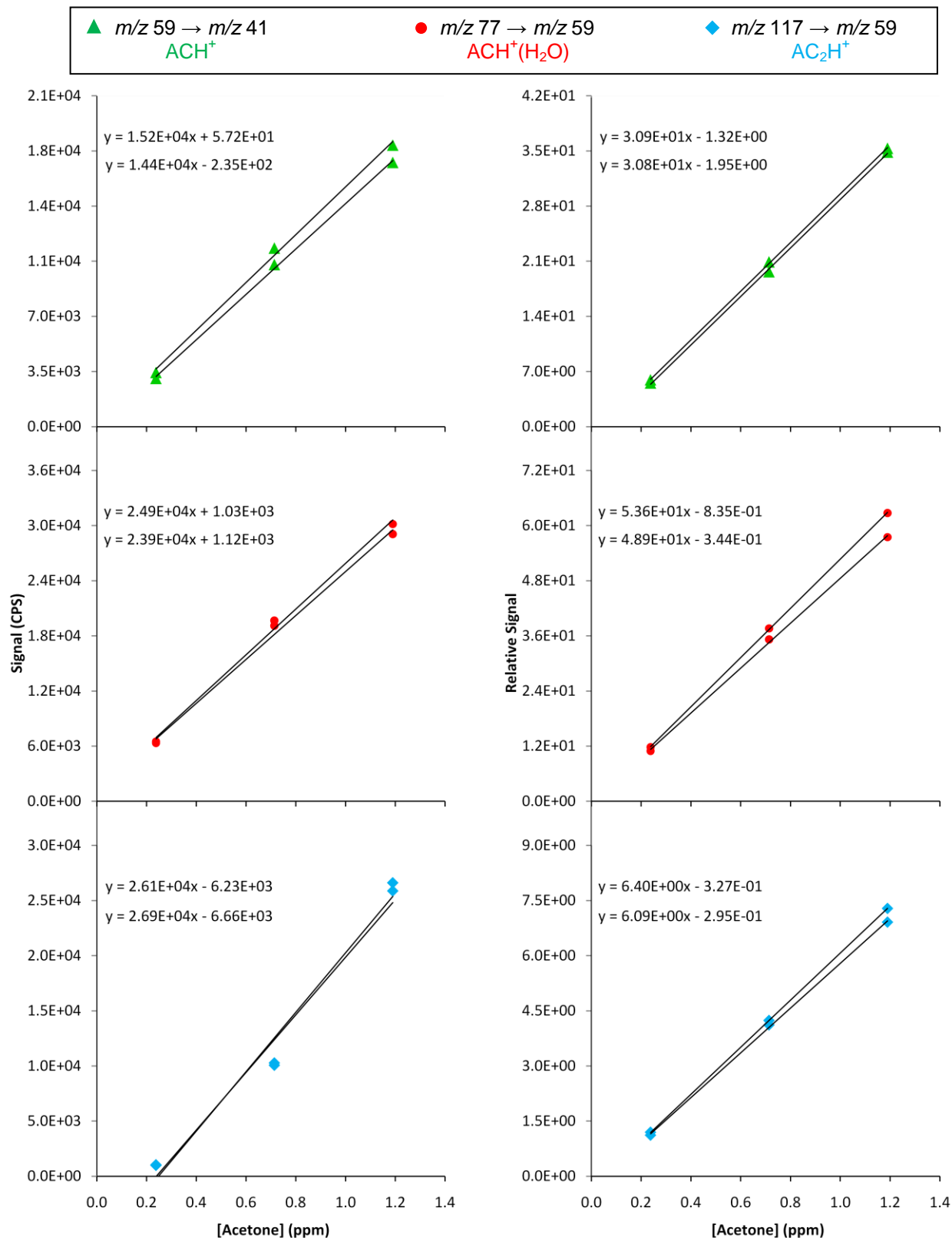
Figure 10: Acetone calibration curves using three precursor → product ion pairs at **20 eV**. Raw signal and relative signal of the acetone pairs are plotted against the concentration of acetone in the left and right pane, respectively. Each graph includes the 1st and 2nd calibration curves. Standard errors are listed in table 7 in the appendix.
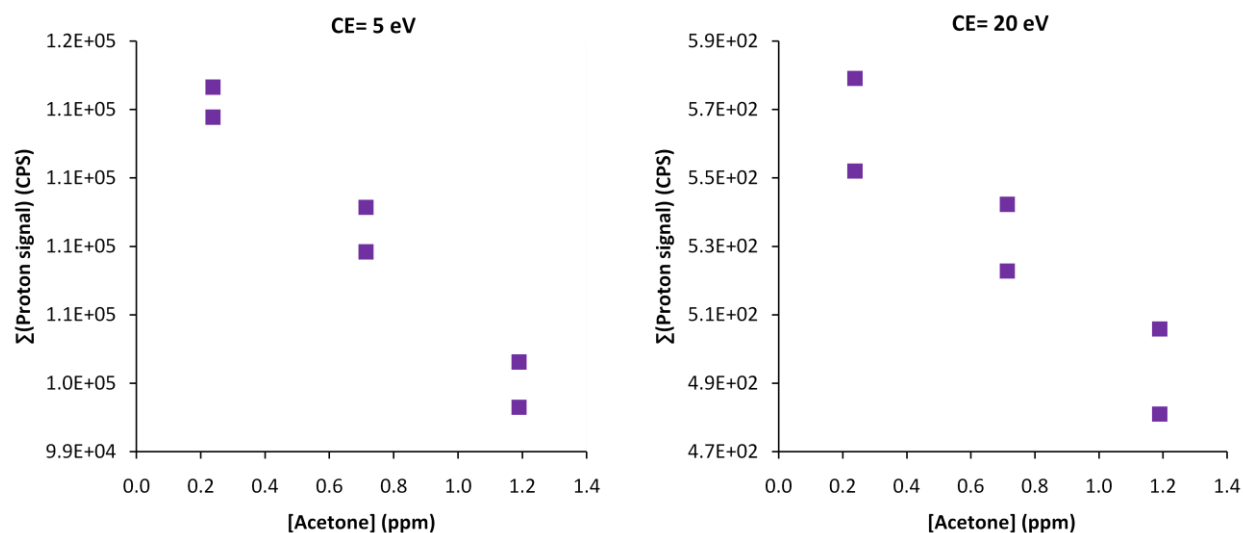
Figure 11: Reduction in the proton signal as the concentration of acetone is increased at 5 and 20 eV.

3.2.3. Control Experiment

An experiment was carried out in order to check the validity of the signal-corrected calibration curves in predicting a known concentration of acetone. For this, 0.43 ppm of acetone were introduced into the flow reactor between the 1st and 2nd calibrations shown in figures 9 and 10. Since cyclohexane was used in excess with the isobutene-O_3 reaction to act as a scavenger, the same amount of cyclohexane, 89 ppm, was introduced into the flow reactor with acetone. The signal of the 0.43 ppm acetone was acquired in the presence and absence of cyclohexane and the concentration was predicted from the calibration curves. The predicted acetone concentration from the calibrations is shown in Figure 12. The bars in figure 12 represent the average predicted concentration from the 1st and 2nd calibration for each of the acetone ions.

It can be clearly observed that in the presence of cyclohexane, the calibrations using AC_2H^+ (*m/z* 117) ion fail to predict the known acetone concentration. The presence of this discrepancy at both 5 and 20 eV, indicates that the concentration of AC_2H^+ ions in the APCI ion

27
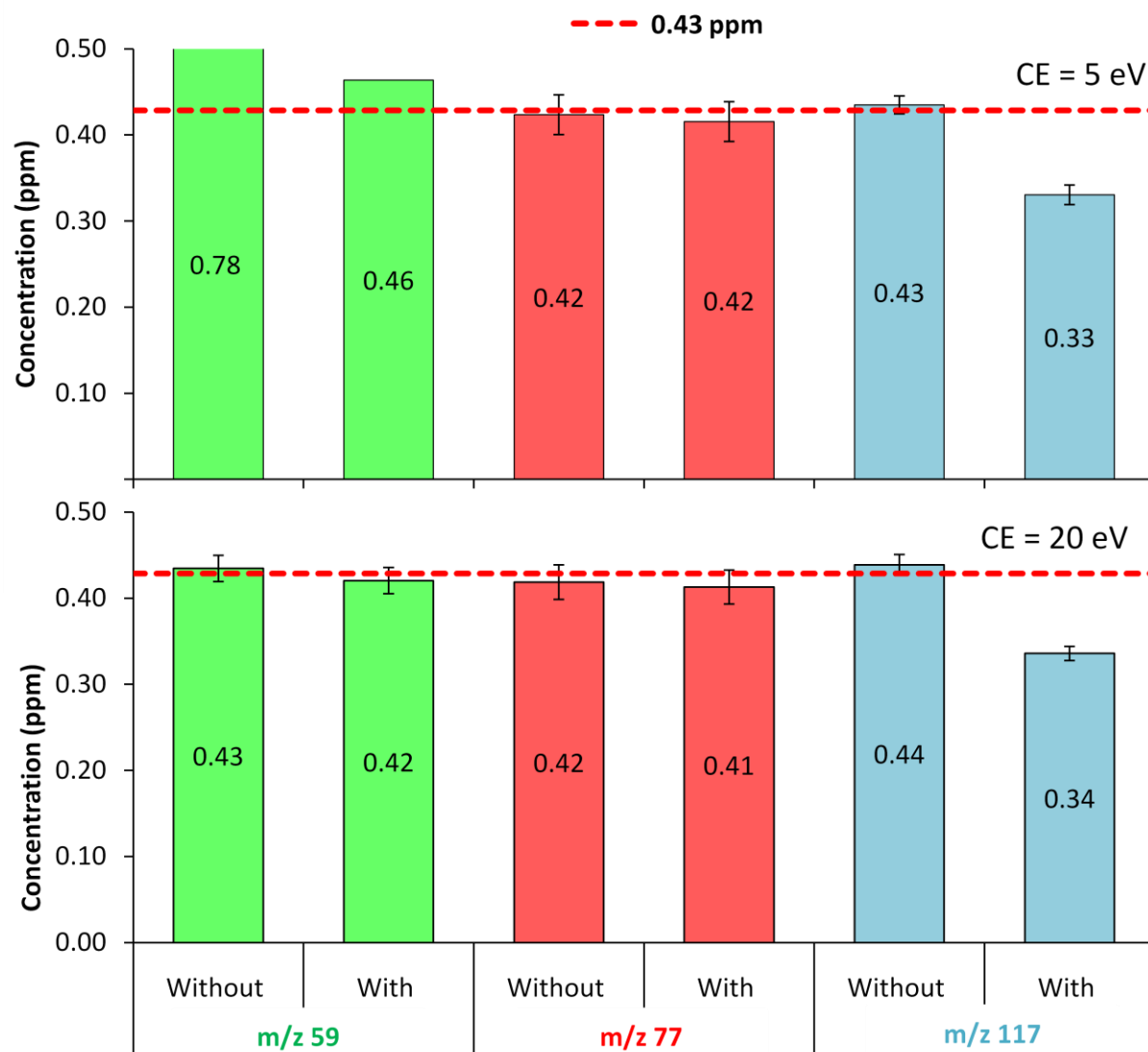
Figure 12: Acetone concentration predictions using the signal-corrected calibration curves in figures 9 and 10, when 0.43 ppm of acetone is introduced in the flow reactor, with/without cyclohexane. Top and bottom bar-graphs are at 5 and 20 eV, respectively. Standard errors are shown.

source might not only be dependent on the reagent ions concentration, but other factors might have an impact on the $[AC_2H^+]$. This also indicates that the derivation of E6 (see section 3.2.1), analogously to E4 derivation, is not applicable and further investigation is required in order to account for all the factors influencing the $[AC_2H^+]$ in the APCI source. As a result, calibrations using AC_2H^+ ion signal were excluded from acetone concentration measurements.

Table 6: 95% confidence limit of the predicted acetone concentration obtained using the signal-corrected calibration curves. Yellow shading indicates where the prediction's 95% confidence range fails to include the known, 0.43 ppm, concentration of acetone.

CE	95% Confidence limit (± ppm)					
	m/z 59		*m/z* 77		*m/z* 117	
	without Cyclohexane	With Cyclohexane	without Cyclohexane	With Cyclohexane	without Cyclohexane	With Cyclohexane
5 eV	2.6E-02	9.4E-05	1.6E-02	1.6E-02	7.4E-03	7.9E-03
20 eV	1.1E-02	1.1E-02	1.4E-02	1.4E-02	8.4E-03	5.8E-03

The acetone concentration measured using ACH^+ (*m/z* 59) calibration at 5 eV is significantly higher than the known concentration (figure 12). In contrast, the calibration at 20 eV for the same ion predicts the concentration with good accuracy. The poor prediction at 5eV could be due the low signal/noise for the ACH^+. Thus, using the ACH^+ calibration at 5 eV was avoided. A "t-test" was carried out in order to determine if the measured acetone concentration is statistically the same as the known concentration, with 95% confidence level. Table 6 lists the 95% confidence limits for all the measured concentrations. It can be deduced that only the ACH^+ (*m/z* 59) at 20 eV and the $ACH^+(H_2O)$ (*m/z* 77) at 5 and 20 eV calibrations were able to predict the actual known concentration of acetone with 95% confidence level in the presence and absence of cyclohexane. Consequently, those calibrations were used for the quantification of acetone produced from the isobutene-O_3 reaction.

3.2.4. Methylglyoxal

Methylglyoxal (MG) is another product formed by the gas phase ozonolysis reaction of isobutene. Attempts were made in order to measure the yield of MG using the same sampling method used for acetone, however, none were successful and MG signal was not detected. That was mainly due to the inability to introduce MG directly into the gas phase by evaporating a solution of MG (40% MG in water) at room temperature.

MG is strongly hygroscopic, and in water, exists largely in the monohydrated (60%) and dihydrated (40%) forms.[15, 16] This indicates that the hydrated forms and not MG were present initially in the solution that was used for MG calibration.

Methylglyoxal diol (MGD)   Methylglyoxal tetrol (MGT)
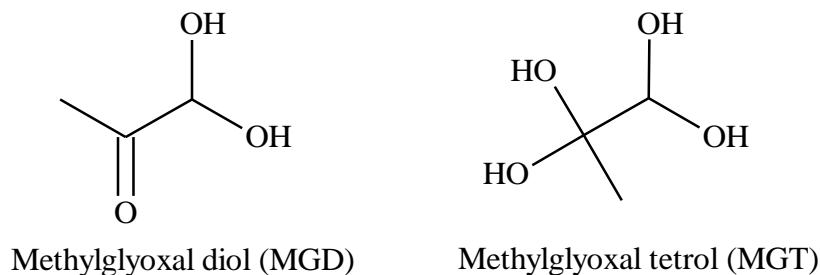
When sampling the MG solution, water evaporation takes place after the droplets are formed in the dilution air flow.[16] Consequently, the concentration of MGD and MGT increases in individual droplets up to a point where a phase change occurs from liquid to solid due to MG oligomerization.[16] The oligomers formed are of low volatility and thus remain in the particle phase.[17] This is the reason why the conventional liquid evaporation method in an air stream was not suitable for MG quantification.

As a result, a modification had to be made in order to better introduce MG into the gas phase for quantitative measurements. For this, a heated nebulizer was added to the experimental set up upstream of the MG solution injection point, inside the APCI ion source. Heating the air stream containing the MG particles, would help increase the volatility of particle phase compounds, which are less volatile at room temperature, and induce pyrolysis of MG oligomers present inside the particles. To test this hypothesis, multiple MG monomer and oligomer related ions were followed by SRM scans, while ramping the temperature of the heated nebulizer.

The MG monomer SRM ion pairs chosen for this experiment were, m/z 73→45, m/z 91→73, m/z 109→73 corresponding to MGH$^+$, MGH$^+$(H$_2$O) and MGH$^+$(H$_2$O)$_2$, respectively.

The last two ion pairs correspond to the water loss fragment of the target ions. Even though the water loss fragment of MGH$^+$ (m/z 73→55) was observed to be the dominant fragment in the MS/MS scan, the ion pair m/z 73→45 was followed instead. That was due to the fact that the water loss fragment of m/z 73 overlapped with the water tetramer H$^+$(H$_2$O)$_4$ target → fragment ion pair, which was present in the background.

As for the MG oligomers, several ions were possible candidates; however, only one MG dimer ion was followed. It was not possible to elucidate the structure of the dimer since its MS/MS scan was at such low intensity that it could hardly be used to distinguish between nominally isobaric hydrated dimers, water clustered dimers and other isomers without the comparison of the obtained fragmentation pattern to that of standards. However, since all possible candidates were oxygen rich species (carbonyl and hydroxyl groups), it was plausible to assume that a loss of water molecule(s) would dominate the MS/MS spectra of those candidates. Therefore, one pair of m/z 181→145, which represents a loss of two water molecules from the target ion 181 m/z, was followed.

By referring to figure 13, one can see that the signal of MG monomers (target ions: m/z 73, 91 and 109) increases with increasing temperature. This increase in signal can be explained by the increasing volatility of MG and its hydrates with temperature. On the other hand, the temperature profile of m/z 181 shows an opposite trend compared to that of the monomers. As mentioned earlier, 181 m/z is a MG dimer related ion and heating may have supplied enough energy to break it apart into MG monomers or other species. Thus, it can be inferred that oligomers decomposition might be another factor contributing to the increase in the monomers signal. Also, a steady state is reached for the three monomer ions between 150°C and 200°C
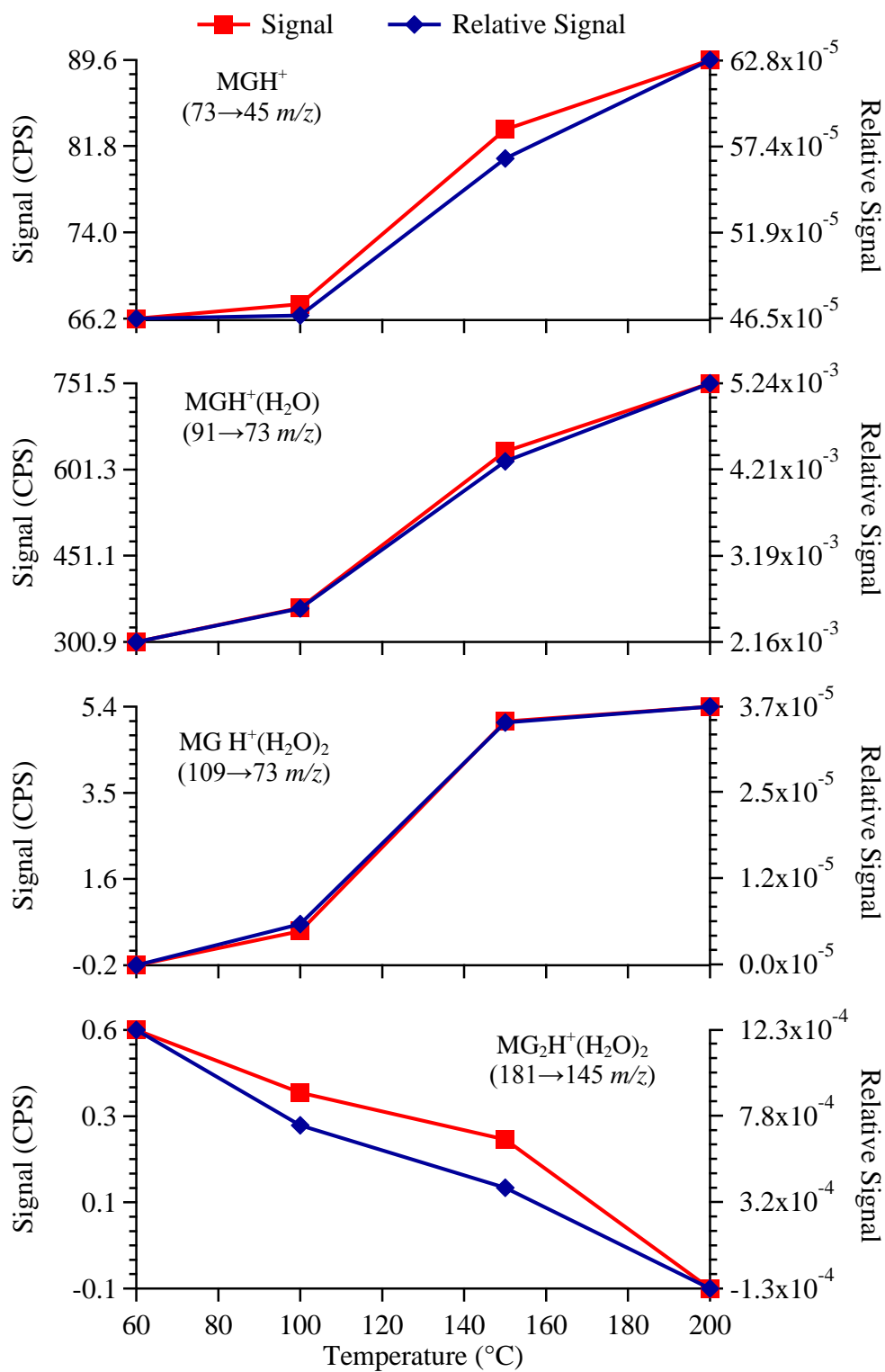
Figure 13: Temperature profile of particle phase MG related ions. The signal and the relative signal to protons are plotted for each ion pair.

indicating an optimum temperature range, where MG concentration reaches a maximum in the gas phase.

It should be noted that the signals of all the ions that were followed in this experiment were considerably low, especially for the *m/z* 181 and 109 ions. Even though the noise in the SRM experiments was very low, it is more reliable to interpret data with higher signal. In order to increase the signal, one can modify the sampling method such that the particles number concentration or the concentration of MGD and MGT per particle increases. Although this was not done in this current study, it could potentially be achieved by performing several of the following modifications. Firstly, forming the particles in highly humid conditions helps in keeping the particles in equilibrium with the gas phase for a considerable amount of time before heating takes place. This can help in reducing MG oligomerization and obtaining a higher concentration of MG hydrates in the particle phase.[16] Secondly, it has been reported that solutions of MG concentration lower than 1 mM have MG aerosol recovery of 19%, while the remaining fraction of MG evaporates.[17] A rapid increase in the MG aerosol recovery is shown for solutions with higher concentration.[17] Thus, by working with very dilute solutions of MG, one can achieve a better evaporation of MG from the particle phase. Lastly, using a Collison nebulizer instead of a syringe for particle production can produce larger number of particles, which subsequently increases the overall MG signal.

3.3. Product Yield

Yield measurements of the isobutene-O_3 reaction products require quantification of both the products and the reagents. Since calibration attempts were only successful with acetone, the yield of this product was evaluated.

3.3.1. Acetone

The yield of acetone was calculated using equation 7,

$$\text{Yield} = \frac{[AC]}{\Delta\,[I]} \tag{E7}$$

where, $[AC]$ is the concentration of acetone and $\Delta[I]$ or $([I]_o - [I]_t)$ is the concentration of isobutene that has been consumed in the reaction. $[AC]$ was obtained from the signal-corrected calibration curves discussed earlier. $\Delta[I]$, however, could not be measured with the APCI-MS and had to be calculated using the integrated rate law for a pseudo first order reaction (E8).

$$\ln\left(\frac{[I]_t}{[I]_o}\right) = -k\,[O_3]\,t_r \tag{E8}$$

$$t_r = \frac{\text{Volume}_{(\text{flow reactor})}}{\text{Flow rate}_{(\text{total})}} \tag{E9}$$

In order to meet pseudo first order conditions, the $[O_3]$ during the reaction of ozone with isobutene, had to remain constant. That was accomplished by ensuring that ozone was present in excess in the reaction, which was performed at concentrations of 15 ppm O_3 and 1.5 ppm $[I]_o$. In E8, $[O_3]$ was measured using the ozone monitor; t is the residence time, which can be calculated using E9, and k is the reaction rate constant, which was obtained from the literature.[18] The initial concentration of isobutene in the flow reactor, $[I]_o$, was calculated based on the flow rates through the two stage dilution system (see appendix for sample calc.). After all these parameters were obtained, the concentration of isobutene at the end of the reaction, $[I]_t$, was evaluated.

It is well known that HO radicals are produced from the gas phase ozonolysis reaction of alkenes.[5, 19-21] The reported HO yield from the reaction of isobutene with ozone is 60%.[19] It was important to scavenge the HO radicals produced, because they are generally far more reactive with alkenes compared to O_3. The presence of HO can introduce bias to the analysis either by: generating new products that are not produced from the ozone reaction or by adding new channels for products that are originally produced from the ozone reaction. In this experiment, cyclohexane was added as a scavenger and the yield of acetone was examined in the presence and absence of this scavenger.

The resultant yield of acetone using the signal-corrected calibration curves of all ions is shown in figure 14. It was determined earlier from the acetone control experiment that calibrations using, m/z 117 at 5 and 20 eV and m/z 59 at 5 eV are not valid for acetone quantification. Still, m/z 59 calibration at 5 eV was used in interpreting the results in figure 14. It can be seen that the yield obtained from m/z 59 at 5 eV in the absence of the HO scavenger is exceedingly higher than the yield obtained with the other ions at the same conditions. Overestimating the yield of acetone was not surprising since the same calibration overestimated the concentration of acetone in the control experiment (Figure 12). It was striking, however, that the percent yield difference between m/z 59 and the other ions was 1600% in the yield experiment, compared to 82% percent difference in the acetone control experiment. The exceptionally high percent difference in the yield experiment for m/z 59 in the absence of cyclohexane was a first indication of a contamination in the m/z 59 → m/z 41 ion pair.

The contamination in the m/z 59 → m/z 41 pair can be inferred also by examining the behaviour of the same ion pair at 20 eV in the absence of cyclohexane. By referring to figure 12,

35
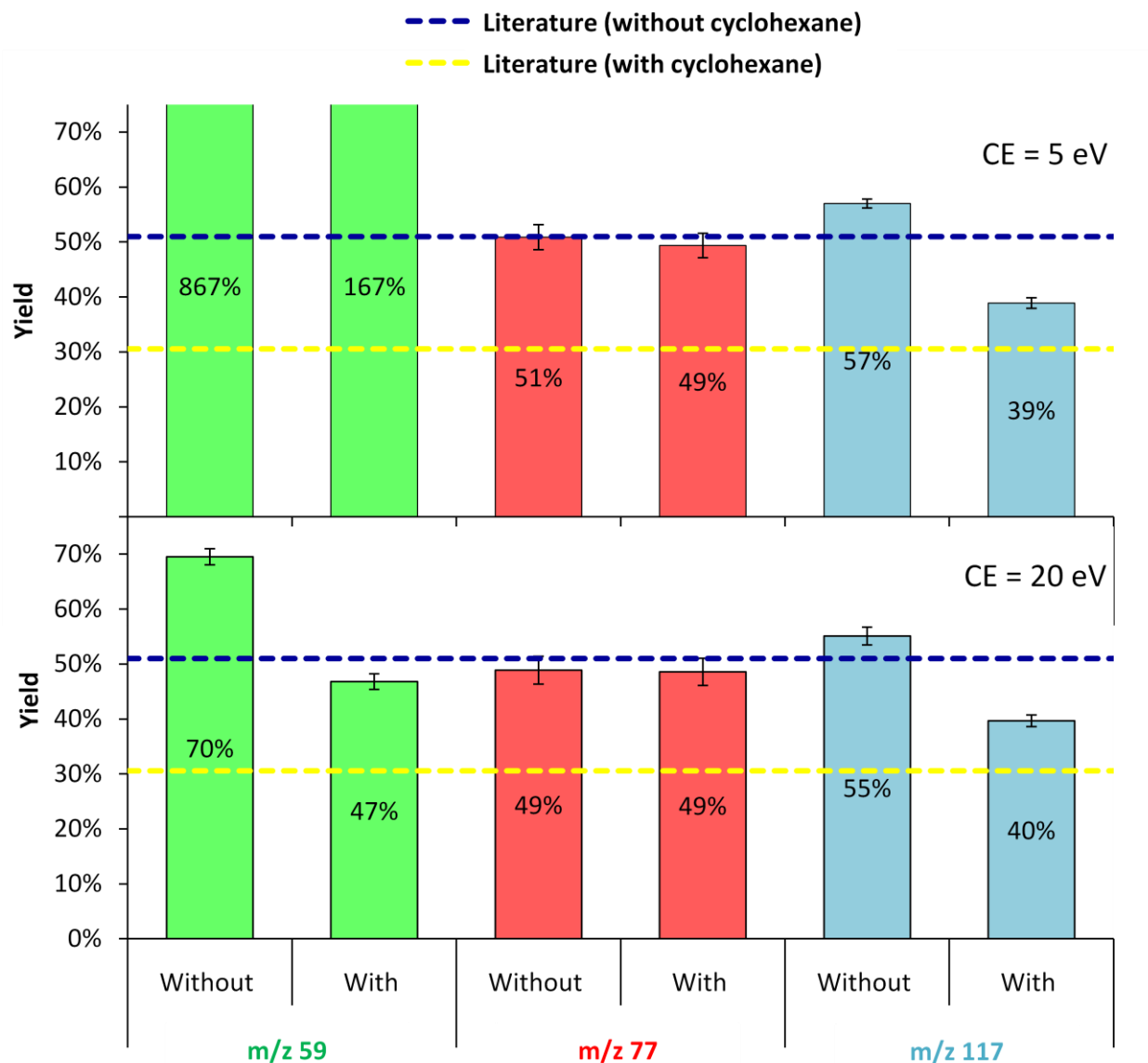
Figure 14: Experimentally measured acetone yield from the gas phase ozonolysis of isobutene compared with literature values in the presence and absence of the HO scavenger, cyclohexane.[1, 5]

the calibrations using all the acetone ion pairs in the absence of cyclohexane were able to predict the concentration of acetone at 20 eV. This means that for the acetone produced from the isobutene-O_3 reaction in the absence of cyclohexane, m/z 59, 77 and 117 should all predict the same acetone concentration (or yield) at 20 eV. Figure 14 shows that the yield obtained using m/z 59 in the absence of cyclohexane (70%) is higher than the corresponding yield of m/z 77 (49%) and m/z 117 (55%). This indicated that there was another product contributing to the SRM

signal at *m/z* 59. Since the APCI-MS sensitivity is compound specific, the concentration of the contaminant could not be evaluated. This contaminant was possibly an isobutene-HO reaction product, because the yield obtained using *m/z* 59 decreases when the HO scavenger is introduced in the flow reactor at 5 and 20 eV.

Due to the contamination of the *m/z* 59 → *m/z* 41 ion pair and the inability to use the *m/z* 117 → *m/z* 59 ion pair for acetone quantification, the only SRM pair that could be used to obtain acetone yield from the isobutene-O_3 reaction was the *m/z* 77 → *m/z* 59 ion pair. Acetone yields obtained at 5 and 20 eV in the absence of cyclohexane for *m/z* 77 were 51% and 49%, respectively. These yields are in agreement within experimental error. The measured yield is also in a good agreement with the one reported in the literature when HO scavenger is absent.[5] In contrast, the second case where cyclohexane was present, the measured yield from this work was 49% at the two collision energies, which is significantly higher than literature reported yield of 31%.[1, 5] These results show that the scavenger had no effect on the yield of acetone. The reason behind the discrepancy between this work and literature was possibly due the different amount of scavenger used in each case. The molar ratio of cyclohexane to the limiting reagent used in this work was 58:1, while the ratio reported in the literature is 1500:1 on average.[5, 6, 21-23] This indicates that the amount of cyclohexane used in this work may not have been sufficient to scavenge all the HO radicals produced. The rate constant for isobutene reaction with HO is approximately 6 orders of magnitude higher than the corresponding reaction with O_3, $5.2*10^{-11}$ and $1.1*10^{-17}$ cm^3 molecule^{-1} s^{-1}, respectively.[18] As a result, the reaction of isobutene with HO proceeds at a considerably faster rate than the reaction with ozone. An expression was derived to measure the fraction of isobutene that reacted with HO to O_3 under the experimental conditions

stated earlier. First, HO reacts with both cyclohexane and isobutene and the fraction of HO

radicals reacting with Isobutene was determined by,

$$[HO]_I \approx \left(\frac{k_{HO-I}[I]}{k_{HO-cyc}[cyc] + k_{HO-I}[I]} \right) \times [HO]$$

Where,

$$[HO] = yield(HO) \times \Delta[I] \approx [HO]_I + [HO]_{cyc}$$

The HO yield (60%) was obtained from the literature.[19] It follows that the ratio Isobutene

reacting with HO to O_3 is,

$$\frac{\Delta[I]_{HO}}{\Delta[I]_{O_3}} \approx \frac{k_{HO-I}[HO]_I}{k_{O_3-I}[O_3]} \approx 2.4 \times 10^4$$

Many assumptions were made in this derivation, including the fact that HO can also react with

isobutene oxidation products. Still, it can be used to obtain a qualitative picture. The ratio shows

that a large fraction of isobutene that was intended to react with ozone had actually reacted with

HO under the experimental conditions used in this work.

More experiments need to be completed in order to test the hypothesis that the amount of

cyclohexane used, was insufficient to scavenge all the HO produced, which led to the observed

discrepancy between the acetone yield obtained in this work and the yield reported in literature.

The following are a few suggestions for future experiments that may shed light on this matter.

First, while the reaction of isobutene with ozone is taking place, one can increase the

concentration of cyclohexane gradually and monitor the yield of acetone. The concentration of

cyclohexane, at which the reduction in acetone yield reaches a steady state, indicates the level

where HO radicals are scavenged completely. Another possible experiment includes using a

different HO scavenger, such as carbon monoxide (CO).[5] CO may be more suitable with the

APCI-MS method of analysis, since unlike what was seen for the cyclohexane oxidation products, the products of the CO-HO reaction do not contribute to the background signal.

4. Conclusion

The results show that on-line VOCs quantification using the APCI-MS/MS is promising, as several limitations encountered previously can be overcome using the correction described in this study. This correction as well as the selectivity provided using the SRM scan allow for VOCs measurement to be completed with high reliability, even in complex matrices. However, care must be taken when choosing the SRM ion pairs to ensure that the signal acquired is unique to the analyte of interest and no interferences are associated with it.

The good agreement between this work and the literature in the acetone yield from the gas phase reaction of ozone with isobutene in the absence of the HO scavenger is an indication of the applicability of the quantification method for on-line yield measurements. Complex ozonolysis reactions involving more atmospherically important alkenes, where gas and particle phase products are produced, can be studied using the flow reactor system used for this work. These results may give a better characterization of alkenes ozonolysis reactions and the products produced, which may lead to better models and provide a basis for control strategies.

Appendix

Table 7: Standard errors associated with calibration curves shown in figures 1 and 2. Yellow shading is an indicative of where higher standard error exists, when the signal and relative signals are compared for one particular precursor ion.

CE	Calibration	[Acetone] (ppm)	Standard error (ppm)					
			m/z 59		m/z 77		m/z 117	
			Signal	Relative	Signal	Relative	Signal	Relative
5 eV	1st	0.238	1.0E-02	3.4E-02	4.3E-02	1.4E-02	1.0E-01	5.2E-03
		0.714	6.9E-03	2.3E-02	2.9E-02	9.3E-03	7.3E-02	3.5E-03
		1.190	1.0E-02	3.5E-02	4.1E-02	1.4E-02	1.1E-01	5.2E-03
	2nd	0.238	2.1E-02	6.3E-03	3.1E-02	3.2E-03	1.0E-01	1.9E-03
		0.714	1.4E-02	4.3E-03	2.1E-02	2.2E-03	7.6E-02	1.3E-03
		1.190	2.0E-02	6.3E-03	3.0E-02	3.2E-03	1.2E-01	1.9E-03
20 eV	1st	0.238	2.1E-02	1.3E-02	4.3E-02	5.3E-03	1.0E-01	4.6E-04
		0.714	1.4E-02	9.2E-03	2.9E-02	3.6E-03	7.6E-02	3.1E-04
		1.190	2.0E-02	1.4E-02	4.1E-02	5.3E-03	1.2E-01	4.6E-04
	2nd	0.238	3.6E-02	6.9E-03	4.7E-02	1.7E-02	9.2E-02	1.3E-02
		0.714	2.4E-02	4.7E-03	3.2E-02	1.1E-02	6.7E-02	9.0E-03
		1.190	3.5E-02	6.9E-03	4.5E-02	1.6E-02	1.0E-01	1.3E-02

Calculations:

- Initial concentration of isobutene in the flow reactor ($[I]_o$):

$$[I]_o = \frac{FR_2}{(FR_1 + FR_2)} \times \frac{FR_4}{(FR_3 + FR_4)} \times \frac{FR_5}{(FR_5 + FR_6)} \times 10^6 = 1.5 \text{ ppm}$$

- Concentration of Acetone (AC) for Calibrations.

$$[AC] = \frac{n_{AC}}{n_{air}} = \frac{\left(\frac{FR_{AC} \times \rho_{AC}}{MW_{AC}}\right)}{\left(\frac{FR^{\circ}_{air} \times P^{\circ}}{T^{\circ} \times R}\right)}$$

FR_{AC} : Acetone syringe flow rate.
ρ_{AC} : Density of Acetone.
MW_{AC} : Molecular weight of Acetone.
FR°_{air} : Flow rate of the dilution AADCO air corrected to standard pressure and temperature.
P°: Standard pressure.
T°: Standard temperature.
R : Gas constant.

References

(1) Calvert, J. G.; Atkinson, R.; Kerr, J. A.; Madronich, S.; Moortgat, G. K.; Wallington, T. J.; Yarwood, G. In *Reactions of Alkenes with O₃;* The Mechanisms of Atmospheric Oxidation of the Alkenes; Oxford University Press: 2000; Vol. 39, pp 172-335.

(2) Auld, J.; Hastie, D. R. *Int. J. Mass Spectrom.* **2009**, *282*, 91-98.

(3) Atkinson, R.; Carter, W. P. L. *Chem. Rev.* **1984**, *84*, 437-470.

(4) Niki, H.; Maker, P. D.; Savage, C. M.; Breitenbach, L. P.; Hurley, M. D. *J. Phys. Chem.* **1987**, *91*, 941-946.

(5) Neeb, P.; Moortgat, G. K. *J. Phys. Chem. A* **1999**, *103*, 9003-9012.

(6) Atkinson, R.; Aschmann, S. M.; Arey, J.; Shorees, B. *J. Geophys. Res. -Atmos.* **1992**, *97*, 6065-6073.

(7) Hunter, E. P. L.; Lias, S. G. *J. Phys. Chem. Ref. Data* **1998**, *27*, 413-656.

(8) Blake, R. S.; Monks, P. S.; Ellis, A. M. *Chem. Rev.* **2009**, *109*, 861-896.

(9) Bennett, J. Flow Reactor Studies of Aromatic Hydrocarbon Photo-Oxidation Products Using On-Line Gas/Particle Separation and MS-MS Analysis, York University, Toronto, Canada, 2010.

(10) Kirmse, W. *Eur. J. Org. Chem.* **2002**, *2002*, 2193-2256.

(11) DeFrees, D. J.; McLean, A. D. *J. Phys. Chem.* **1982**, *86*, 2835-2837.

(12) Nicol, G.; Sunner, J.; Kebarle, P. *Int. J. Mass Spectrom. Ion Processes* **1988**, *84*, 135-155.

(13) Sunner, J.; Nicol, G.; Kebarle, P. *Anal. Chem.* **1988**, *60*, 1300-1307.

(14) Sunner, J.; Ikonomou, M. G.; Kebarle, P. *Anal. Chem.* **1988**, *60*, 1308-1313.

(15) Krizner, H. E.; De Haan, D. O.; Kua, J. *J. Phys. Chem. A* **2009**, *113*, 6994-7001.

(16) Loeffler, K. W.; Koehler, C. A.; Paul, N. M.; De Haan, D. O. *Environ. Sci. Technol.* **2006**, *40*, 6318-6323.

(17) De Haan, D. O.; Corrigan, A. L.; Tolbert, M. A.; Jimenez, J. L.; Wood, S. E.; Turley, J. J. *Environ. Sci. Technol.* **2009**, *43*, 8184-8190.

(18) Atkinson, R. *J. Phys. Chem. Ref. Data* **1997**, *26*, 215-290.

(19) Wegener, R.; Brauers, T.; Koppmann, R.; Rodriguez Bares, S.; Rohrer, F.; Tillmann, R.; Wahner, A.; Hansel, A.; Wisthaler, A. *J. Geophys. Res. -Atmos.* **2007**, *112*, D13301.

(20) Paulson, S. E.; Chung, M. Y.; Hasson, A. S. *J Phys Chem A* **1999**, *103*, 8125-8138.

(21) Rickard, A. R.; Johnson, D.; McGill, C. D.; Marston, G. *J Phys Chem A* **1999**, *103*, 7656-7664.

(22) Tuazon, E. C.; Aschmann, S. M.; Arey, J.; Atkinson, R. *Environ. Sci. Technol.* **1997**, *31*, 3004-3009.

(23) Atkinson, R.; Aschmann, S. M. *Environ. Sci. Technol.* **1993**, *27*, 1357-1363.